IOP Conference Series: Materials Science and Engineering

Experimental determination of dynamic parameters of an industrial robot

IOP Conf. Series: Materials Science and Engineering **227** (2017) 012012 doi:10.1088/1757-899X/227/1/012012

Experimental determination of dynamic parameters of an industrial robot

W Banas[1], **G Cwikła**[2], **K Foit**[3], **A Gwiazda**[4], **Z Monica**[5] **and A Sekala**[6]
[1-6]Silesian University of Technology, Faculty of Mechanical Engineering, Institute of Engineering Processes Automation and Integrated Manufacturing Systems, Konarskiego 18A, 44-100 Gliwice, Poland

E-mail: waclaw.banas@polsl.pl

Abstract. In an industry increasingly used are industrial robots. Commonly used are two basic methods of programming, on-line programming and off-line programming. In both cases, the programming consists in getting to the selected points record this position, and set the order of movement of the robot, and the introduction of logical tests. Such a program is easy to write, and it is suitable for most industrial applications. Especially when the process is known, respectively slow and unchanging. In this case, the program is being prepared for a universal model of the robot with the appropriate geometry and are checked only collisions. Is not taken into account the dynamics of the robot and how it will really behave while in motion. For this reason, the robot programmed to be tested at a reduced speed, which is raised gradually to the final value. Depending on the complexity of the move and the proximity of the elements it takes a lot of time. It is easy to notice that the robot at different speeds have different trajectories and behaves differently.

1. Introduction

It is easy to determine in theory, geometric and mass parameters of robot arm separately but the determination of the parameters for the whole of robot is not so easy and requires a series of experiments. When determining mass parameters it is necessary to know the material from which it was made [16, 17]

These experiments were carried out on the robot Fanuc Arc Mate using a very fast real-time computer – PXI [3, 4]. The robot is a typical welding robot but equipped with appropriate sensors to enable testing. Sensors measure the movement parameters and electrical parameters of work of individual drives. The results are sent to the real-time computer and stored there. After the recording is analyzed of movement parameters of each arm and drives the robot. When this is done in a variety of configurations robot is possible to determine the dynamic parameters of individual drives and robot arm. The vision system could support this process [13, 14].

It is very difficult to carry out such experiments. Firstly, when the robot does not move automatically, the brakes are activated, which makes it impossible to perform the experiments. It is very difficult to carry out such experiments. Firstly, when the robot does not move automatically, the brakes are activated, which makes it impossible to perform the experiments. Secondly, the robot moves all axes in motion while it controls its speed and changes all the time [8]. Thirdly, each servo drive has speed ramps to make the movements smooth, but this makes it difficult to analyze. The best

for analysis would be with impulse forcing. Such an impulse is during an emergency stop, but is triggered by the brakes.

2. Measurements of dynamic parameters of a robot

After many tests, method of forcing similar to the impulse was found. Many measurements were taken, because the difficulty of the forcing method, not all results were satisfactory.

Of the correct tests, one was selected for further analysis. Figures 1-6 shows the results of measurements on all joints of a robot.

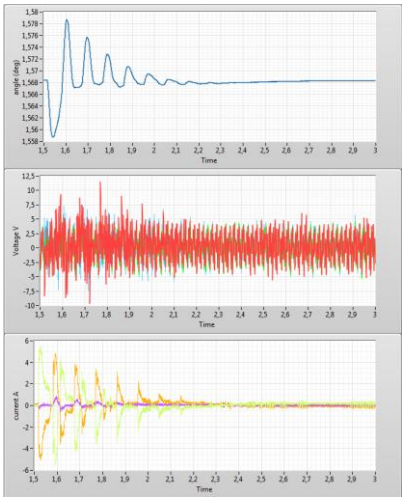

Figure 1. Angle displacement and Voltage and current of joint 1.

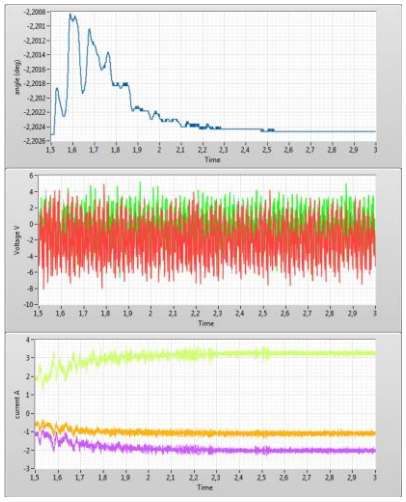

Figure 2. Angle displacement and Voltage and current of joint 2.

It is easy to note in figure 1 that the angular displacement has a plot similar to the damped vibrations but the asymptote is not centered and the lower part of the amplitudes is cuted. Voltage graphs show peaks that protrude over the voltages over time. The graph of current changes is more interesting because of the nature of the waveform.

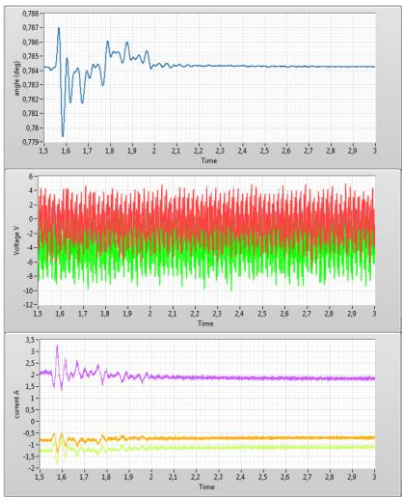

Figure 3. Angle displacement and Voltage and current of joint 3.

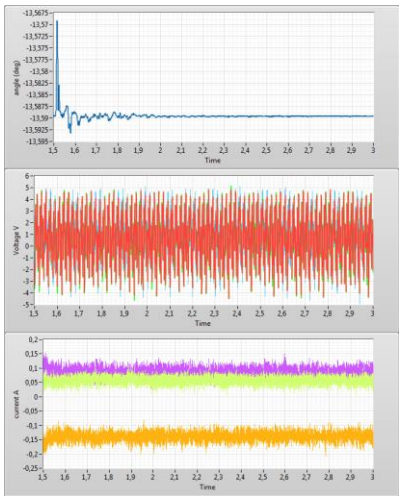

Figure 4. Angle displacement and Voltage and current of joint 4.

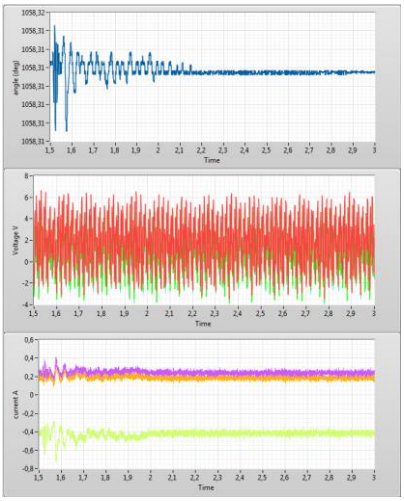

Figure 5. Angle displacement and Voltage and current of joint 5.

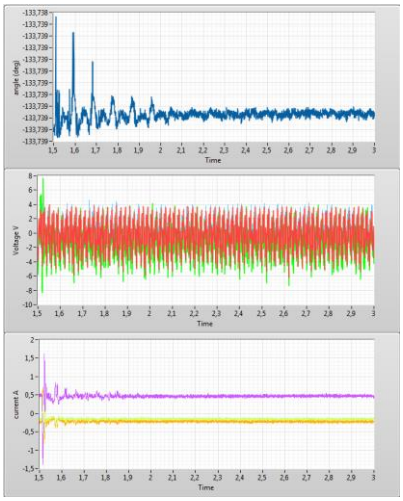

Figure 6. Angle displacement and Voltage and current of joint 6.

In figures 2, 4, 5 and 6 the angular displacements have nonlinearities that are probably caused by joints clearance. On these charts it is hard to notice the change in voltage. During experiments the biggest problems were joints 4 and 6 because of their construction.

After analysing graphs figures 1-6, the angles and currents were taken into the analysis.

3. Analysis of waveforms

The research was done in Labview the same way in which data acquisition was done. Because the analysis was made from the data stored in the file, it was not necessary to use a real-time computer and could use an ordinary PC, but the program could also be apply on a PXI computer [14].

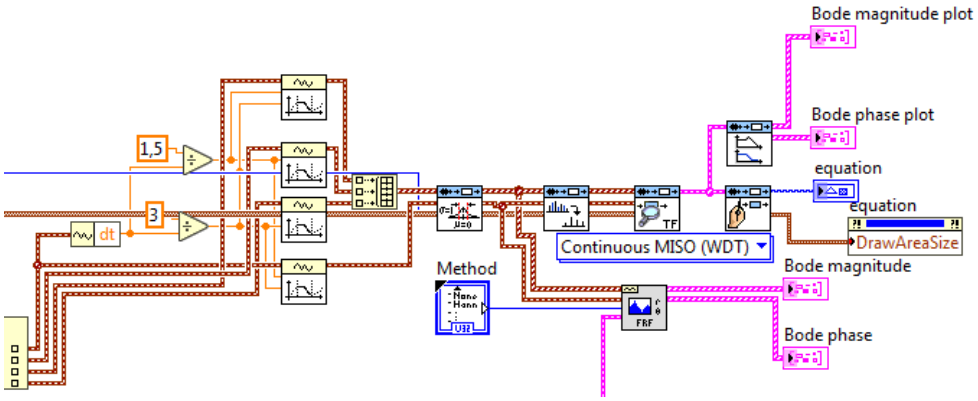

Figure 7. Part of the program for the calculation of dynamic parameters.

Sampling time is 0.25 ms that is 4000 samples per second. During this time, the PXI computer makes measurements and writes them to the file.

This causes high frequencies to dominate the system, so data preparation was necessary [6, 7]. The part of the program where pre-processing is performed followed by the model analysis is shown in figure 7.

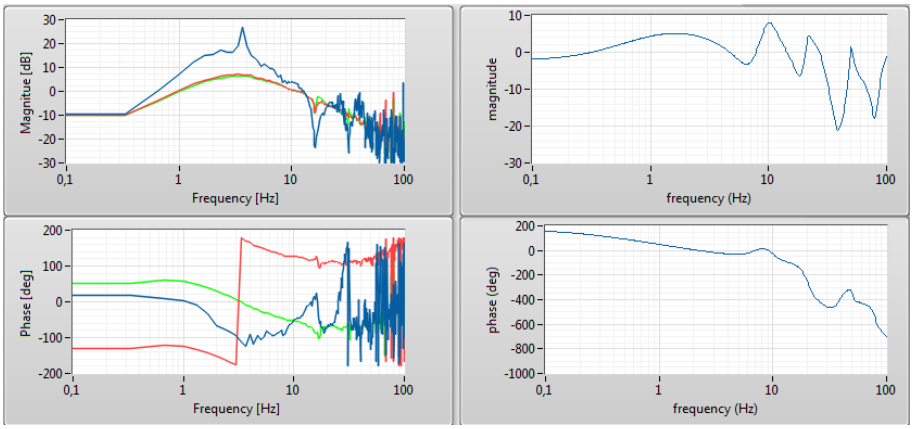

Figure 8. Bode plots of joint 1.

Figure 8 shows the Bode characteristic of the experiment and the approximated function described in figure 9.

$$y(s) = \left[\frac{-0{,}778697 + 0{,}342373s + 0{,}00377167s^2 + 0{,}000239814s^3 + 9{,}51237E\text{-}7s^4 + 2{,}917E\text{-}8s^5 + 7{,}77241E\text{-}11s^6 + 1{,}32588E\text{-}12s^7}{1 + 0{,}205878s + 0{,}0102584s^2 + 0{,}000179871s^3 + 3{,}8184E\text{-}6s^4 + 3{,}3671E\text{-}8s^5 + 3{,}59124E\text{-}10s^6 + 2{,}08124E\text{-}12s^7} \right.$$

$$\frac{-0{,}12469 + 0{,}351219s - 0{,}010297s^2 + 0{,}000165181s^3 - 8{,}83915E\text{-}6s^4 + 7{,}12374E\text{-}9s^5 - 1{,}98421E\text{-}9s^6 - 3{,}13998E\text{-}12s^7}{1 + 0{,}13365s + 0{,}00769689s^2 + 0{,}000251625s^3 + 6{,}10319E\text{-}6s^4 + 1{,}22033E\text{-}7s^5 + 1{,}44747E\text{-}9s^6 + 1{,}9566E\text{-}11s^7}$$

$$\left. \frac{0{,}477633 + 0{,}261753s + 0{,}0022517s^2 + 0{,}000290516s^3 + 5{,}51838E\text{-}7s^4 + 6{,}78836E\text{-}8s^5 + 2{,}14628E\text{-}10s^6 + 3{,}68041E\text{-}12s^7}{1 + 0{,}0834478s + 0{,}00513948s^2 + 0{,}000167915s^3 + 4{,}83106E\text{-}6s^4 + 6{,}25205E\text{-}8s^5 + 9{,}76223E\text{-}10s^6 + 4{,}61384E\text{-}12s^7} \right] u(s)$$

Figure 9. Transfer function joint 1.

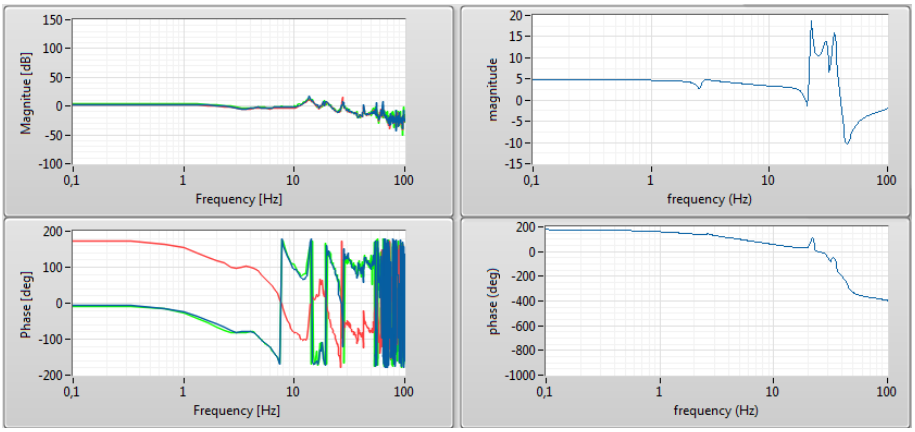

Figure 10. Bode plots of joint 2.

It is very difficult to obtain the same characteristics as obtained from the real system. These are just approximations and the choice between the accuracy of the mapping and the degree of the equation of the transition function. In CAD modelling and simulation, machine mechanisms are more important than lower frequencies [10, 11].

$$y(s) = \left[\frac{-1{,}73239 + 0{,}0276834s - 0{,}00638321s^2 + 0{,}000139099s^3 - 4{,}3491E\text{-}7s^4 + 1{,}31449E\text{-}8s^5 - 4{,}52461E\text{-}12s^6}{1 + 0{,}0382036s + 0{,}00404648s^2 + 0{,}000122004s^3 + 7{,}37507E\text{-}7s^4 + 1{,}20324E\text{-}8s^5 + 4{,}32053E\text{-}11s^6} \right.$$

$$\frac{-3{,}15823 - 0{,}172924s - 0{,}0166851s^2 + 4{,}76048E\text{-}5s^3 - 6{,}66853E\text{-}6s^4 + 4{,}94277E\text{-}9s^5 - 6{,}25372E\text{-}10s^6}{1 + 0{,}0854243s + 0{,}0092697s^2 + 0{,}000117243s^3 + 5{,}88118E\text{-}6s^4 + 2{,}58473E\text{-}8s^5 + 7{,}25257E\text{-}10s^6 + 1{,}76023E\text{-}12s^7}$$

$$\left. \frac{-0{,}261861 - 0{,}0161413s + 0{,}00186889s^2 - 9{,}38911E\text{-}6s^3 + 1{,}25131E\text{-}6s^4 - 1{,}72725E\text{-}9s^5 + 2{,}637E\text{-}10s^6}{1 + 0{,}0404528s + 0{,}00333589s^2 + 4{,}64143E\text{-}5s^3 + 1{,}83856E\text{-}6s^4 + 1{,}52786E\text{-}8s^5 + 3{,}76654E\text{-}10s^6 + 1{,}95749E\text{-}12s^7} \right] \mathbf{u}(s)$$

Figure 11. Transfer function joint 2.

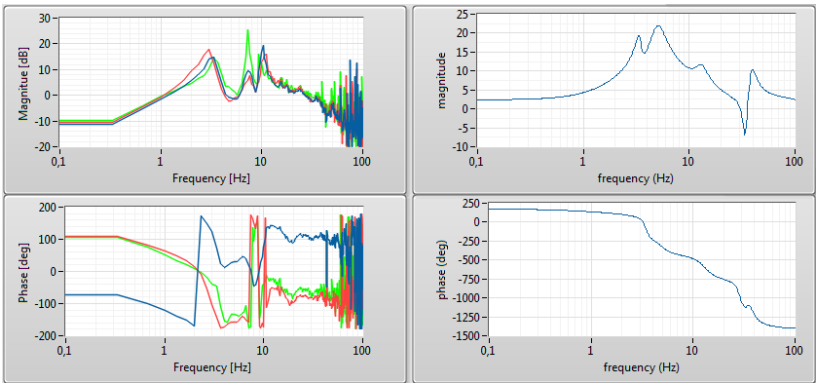

Figure 12. Bode plots of joint 3.

$$y(s) = \left[\frac{-1{,}31545 + 0{,}140859s - 0{,}00349332s^2 + 0{,}000273884s^3 + 2{,}58251E\text{-}7s^4 + 3{,}53906E\text{-}8s^5 + 4{,}14493E\text{-}10s^6 + 1{,}07707E\text{-}12s^7}{1 + 0{,}0224317s + 0{,}00359657s^2 + 5{,}47474E\text{-}5s^3 + 3{,}16734E\text{-}6s^4 + 2{,}53968E\text{-}8s^5 + 5{,}8013E\text{-}10s^6 + 2{,}61724E\text{-}12s^7} \right.$$

$$\frac{-2{,}96821 + 0{,}0821583s - 0{,}00251182s^2 + 4{,}01723E\text{-}5s^3 - 6{,}59205E\text{-}7s^4 + 5{,}78516E\text{-}9s^5 - 6{,}40253E\text{-}11s^6}{1 + 0{,}0265281s + 0{,}00135105s^2 + 2{,}31751E\text{-}5s^3 + 5{,}61787E\text{-}7s^4 + 6{,}29223E\text{-}9s^5 + 9{,}14694E\text{-}11s^6}$$

$$\left. \frac{2{,}26828 - 0{,}2112s + 0{,}0202598s^2 - 0{,}00067176s^3 + 4{,}66004E\text{-}5s^4 - 4{,}05646E\text{-}7s^5 + 1{,}72535E\text{-}8s^6 - 8{,}05763E\text{-}11s^7 + 2{,}4326E\text{-}12s^8}{1 + 0{,}147343s + 0{,}0177902s^2 + 0{,}00060098s^3 + 3{,}12901E\text{-}5s^4 + 5{,}55525E\text{-}7s^5 + 1{,}53329E\text{-}8s^6 + 1{,}73013E\text{-}10s^7 + 2{,}56978E\text{-}12s^8} \right] \mathbf{u}(s)$$

Figure 13. Transfer function joint 3.

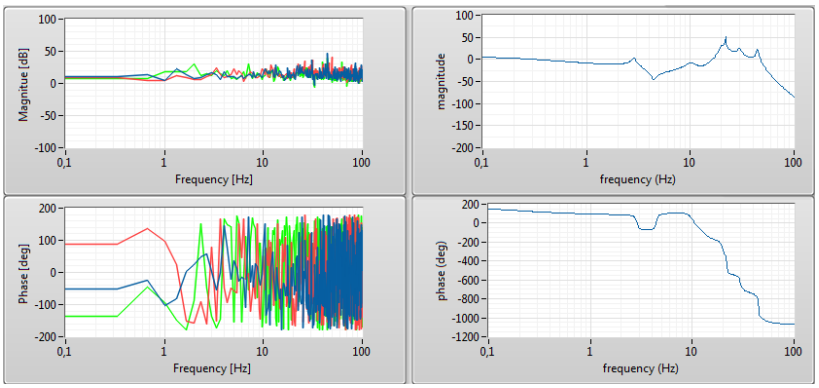

Figure 14. Bode plots of joint 4.

$$y(s) = \left[\frac{-1{,}97374 + 0{,}00318768s - 0{,}0023117s^2 + 4{,}60716E\text{-}5s^3 + 3{,}15295E\text{-}7s^4 + 5{,}34911E\text{-}8s^5 - 4{,}63043E\text{-}11s^6 + 7{,}56988E\text{-}12s^7}{1 + 0{,}888979s + 0{,}0103881s^2 + 0{,}00311807s^3 + 1{,}51773E\text{-}5s^4 + 1{,}20602E\text{-}6s^5 + 3{,}41058E\text{-}9s^6 + 1{,}49533E\text{-}10s^7} \right.$$

$$\frac{-20{,}3876 - 1{,}35816s - 0{,}027776s^2 - 8{,}79934E\text{-}5s^3 + 5{,}98917E\text{-}5s^4 + 5{,}25918E\text{-}7s^5 + 9{,}74452E\text{-}9s^6 + 7{,}90135E\text{-}11s^7}{1 + 6{,}72318s + 0{,}435447s^2 + 0{,}0267923s^3 + 0{,}00047082s^4 + 8{,}8857E\text{-}6s^5 + 1{,}02898E\text{-}7s^6 + 9{,}90273E\text{-}10s^7 + 7{,}62422E\text{-}12s^8}$$

$$\left. \frac{-0{,}126182 + 0{,}00320552s - 9{,}55183E\text{-}5s^2 + 2{,}81659E\text{-}6s^3 - 1{,}63268E\text{-}8s^4 + 6{,}81789E\text{-}10s^5}{1 + 0{,}0151446s + 0{,}00111446s^2 + 1{,}18366E\text{-}5s^3 + 3{,}7149E\text{-}7s^4 + 2{,}89954E\text{-}9s^5 + 4{,}7858E\text{-}11s^6} \right] \mathbf{u}(s)$$

Figure 15. Transfer function joint 4.

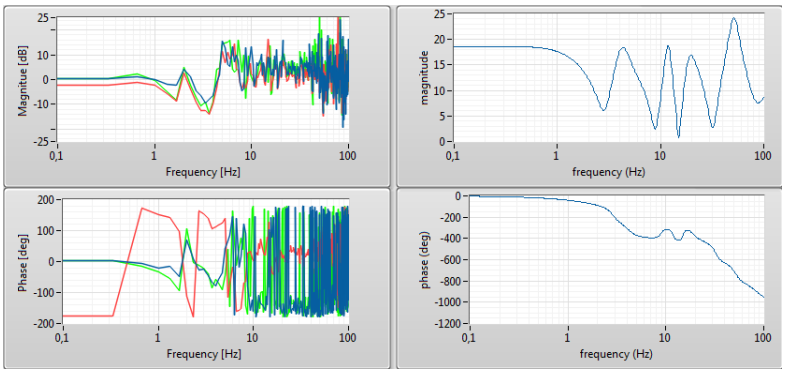

Figure 16. Bode plots of joint 5.

$$y(s) = \left[\frac{8{,}54124 + 1{,}41508s + 0{,}0481214s^2 + 0{,}00605154s^3 + 0{,}000139276s^4 + 6{,}56996E\text{-}6s^5 + 8{,}48627E\text{-}8s^6 + 2{,}28088E\text{-}9s^7 + 1{,}67723E\text{-}11s^8}{1 + 0{,}264042s + 0{,}0269441s^2 + 0{,}00138572s^3 + 6{,}28199E\text{-}5s^4 + 1{,}64962E\text{-}6s^5 + 4{,}00459E\text{-}8s^6 + 5{,}81882E\text{-}10s^7 + 8{,}48537E\text{-}12s^8} \right.$$

$$\frac{-0{,}375996 - 0{,}946612s - 0{,}0403944s^2 - 0{,}00261033s^3 - 7{,}80488E\text{-}5s^4 - 1{,}95461E\text{-}6s^5 - 3{,}77556E\text{-}8s^6 - 5{,}74689E\text{-}10s^7 - 6{,}55031E\text{-}12s^8}{1 + 0{,}947776s + 0{,}116623s^2 + 0{,}00431797s^3 + 0{,}000229754s^4 + 4{,}20424E\text{-}6s^5 + 1{,}17376E\text{-}7s^6 + 1{,}39182E\text{-}9s^7 + 2{,}08942E\text{-}11s^8}$$

$$\left. \frac{4{,}24915 + 0{,}211517s + 0{,}0270152s^2 + 0{,}000171514s^3 + 4{,}38893E\text{-}5s^4 - 1{,}80326E\text{-}7s^5 + 1{,}93092E\text{-}8s^6 - 4{,}55295E\text{-}11s^7 + 2{,}74909E\text{-}12s^8}{1 + 0{,}136394s + 0{,}0211993s^2 + 0{,}000950745s^3 + 4{,}32751E\text{-}5s^4 + 1{,}07953E\text{-}6s^5 + 2{,}47277E\text{-}8s^6 + 3{,}09285E\text{-}10s^7 + 4{,}50508E\text{-}12s^8} \right] \mathbf{u}(s)$$

Figure 17. Transfer function joint 5.

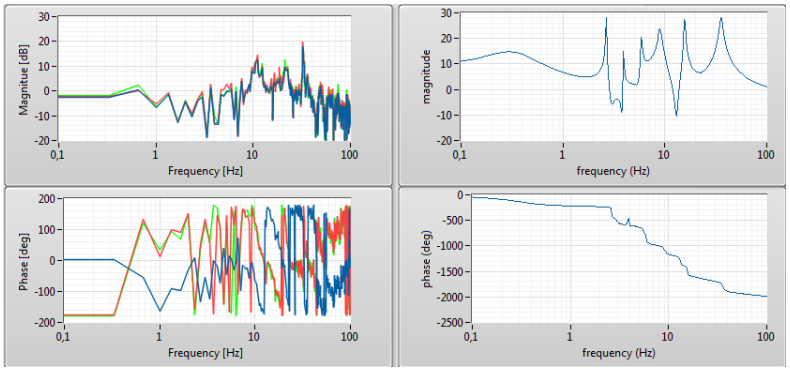

Figure 18. Bode plots of joint 6.

$$y(s) = \left[\frac{3,06896 - 2,25202s - 0,18174s^2 - 0,00306912s^3 - 0,00128319s^4 + 2,97395E\text{-}5s^5 - 2,74183E\text{-}6s^6 + 7,53956E\text{-}8s^7 - 2,24286E\text{-}9s^8 + 5,0148E\text{-}11s^9}{1 + 0,556464s + 0,256516s^2 + 0,00451268s^3 + 0,00162259s^4 + 1,25503E\text{-}5s^5 + 3,12241E\text{-}6s^6 + 1,46775E\text{-}8s^7 + 2,22028E\text{-}9s^8 + 6,92902E\text{-}12s^9} \right.$$

$$\frac{0,532239 - 0,163712s - 0,0192757s^2 - 0,00141971s^3 + 1,87686E\text{-}5s^4 - 5,26119E\text{-}6s^5 + 1,88145E\text{-}7s^6 - 4,51177E\text{-}9s^7 + 1,91239E\text{-}10s^8}{1 + 0,0830177s + 0,0387733s^2 + 0,00110975s^3 + 0,000189361s^4 + 3,57551E\text{-}6s^5 + 2,66427E\text{-}7s^6 + 3,62832E\text{-}9s^7 + 1,33236E\text{-}10s^8 + 1,29591E\text{-}12s^9}$$

$$\left. \frac{-7,71165 - 0,691577s - 0,485658s^2 - 0,0274091s^3 - 0,00203379s^4 - 3,73393E\text{-}5s^5 - 2,5269E\text{-}6s^6 + 2,22676E\text{-}8s^7 - 1,22388E\text{-}9s^8 + 2,46338E\text{-}11s^9}{1 + 0,0573939s + 0,0793652s^2 + 0,00371054s^3 + 0,000398184s^4 + 1,26318E\text{-}5s^5 + 5,6332E\text{-}7s^6 + 1,24788E\text{-}8s^7 + 2,80722E\text{-}10s^8 + 4,40334E\text{-}12s^9} \right] \mathbf{u}(s)$$

Figure 19. Transfer function joint 6.

The obtained Bode characteristics and transfer function in the same position in different experiments were similar, so the results obtained from one of the experiments. This enables better CAD [12, 13] robot modelling. The model, which better describes the operation of the production machine, supports modelling the whole system [5, 15].

4. Conclusions

The obtained characteristics are for a particular robot position, but even their designation is a complex process. When determining the dynamic parameters of a whole robot it is difficult to isolate the influence of each element of the robot. Research each item separately facilitate disassembly robot arm robot. Another option is to unlock only one brake and carry out the test successively for all drives. Another option is to unlock only one brake and carry out the test successively for all drives. Both methods require significant interference in the construction and control of the robot.
The research will be developed and their results published.

5. References

[1] Banaś W, Sękala A, Gwiazda A, Foit K, Hryniewicz P and Kost G 2015 Determination of the robot location in a workcell of a flexible production line. *IOP Conf. Ser.: Mater. Sci. Eng.* **95** 012105
[2] Banaś W, Sękala A, Gwiazda A, Foit K, Hryniewicz P and Kost G 2015 The modular design of robotic workcells in a flexible production line. *IOP Conf. Ser.: Mater. Sci. Eng.* **95** 012099
[3] Cholewa A, Świder J, Zbilski A 2016 Numerical model of Fanuc AM100iB robot *IOP Conf. Ser.: Mater. Sci. Eng.* **145** 052002
[4] Cholewa A, Świder J, Zbilski A 2016 Verification of forward kinematics of the numerical and analytical model of Fanuc AM100iB robot *IOP Conf. Ser.: Mater. Sci. Eng.* **145** 052001
[5] Ćwikła G, Krenczyk D, Kampa A and Gołda G 2015 Application of the MIAS methodology in design of the data acquisition system for wastewater treatment plant. *IOP Conf. Ser.: Mater. Sci. Eng.* **95** 012153
[6] Dzitkowski T and Dymarek A 2015 Method of active and passive vibration reduction of synthesized bifurcated drive systems of machines to the required values of amplitudes. *Journal of Vibroengineering* **17(4)** 1578-1592
[7] Dymarek A and Dzitkowski T 2016 Inverse task of vibration active reduction of Mechanical Systems *Mathematical Problems in Engineering* ID 3191807
[8] Foit K and Ćwikła G 2017 The CAD drawing as a source of data for robot programming purposes - a review. *MATEC Web of Conferences* **94** UNSP 05002
[9] Herbuś K and Ociepka P 2016 *IOP Conf. Ser.: Mater. Sci. Eng.,* **145** 042018
[10] Herbuś K and Ociepka P 2016 *IOP Conf. Ser.: Mater. Sci. Eng.,* **145** 052010
[11] Herbuś K and Ociepka P 2015 *IOP Conf. Ser.: Mater. Sci. Eng.* **95** 012096
[12] Herbuś K and Ociepka P 2015 *IOP Conf. Ser.: Mater. Sci. Eng.* **95** 012084

[13] Hryniewicz P, Banaś W, Sękala A, Gwiazda A, Foit K and Kost G 2015 Object positioning in storages of robotized workcells using LabVIEW. Vision *IOP Conf. Ser.: Mater. Sci. Eng.* **95** 012098
[14] Hryniewicz P, Banaś W, Sękala A, Gwiazda A, Foit K and Kost G 2015 Technological process supervising using vision systems cooperating with the LabVIEW vision builder. *IOP Conf. Ser.: Mater. Sci. Eng.* **95** 012086
[15] Skołud B, Krenczyk D, Kalinowski K, Ćwikła G and Grabowik C 2016 Integration of manufacturing functions for SME. *Holonic based approach. Advances in Intelligent Systems and Computing* **527** (Springer) 464-473
[16] Grajcar A, Kciuk M, Topolska S and Płachcińska A Microstructure and Corrosion Behavior of Hot-Deformed and Cold-Strained High-Mn Steels *Journal Of Materials Engineering And Performance* **25(6)**
[17] Topolska S and Labanowski J Impact-Toughness Investigations Of Duplex Stainless Steels *Materiali In Tehnologije* **49(4)** 481-486